Journal of Science and Technology, Vol. 43, No. 1 (2025), pp 88-102

https://dx.doi.org/10.4314/just.v43i1.7

DETERMINATION OF AMBIENT DOSE EQUIVALENT USING A MICROPROCESSOR-CONTROLLED UNIVERSAL REFERENCE-CLASS DOSEMETER

Collins Kafui Azah[1,2]*, Daniel Nii Adjei[1], Philip Deatanyah[1,2], Samuel Osei[1], Prince Marcus Appiah[1], Joseph Kwabena Amoako[2], Frederick Sam[3], Christiana Subaar[4] and Anthony Selorm Kwesi Amable[5]

[1]Radiation Protection Institute, Ghana Atomic Energy Commission, Legon, Accra, Ghana
[2]Department of Nuclear Safety and Security, Graduate School of Nuclear and Allied Sciences, University of Ghana, Kwabenya, Accra, Ghana
[3]Department of Physics, University of Cape Coast, Cape Coast, Ghana
[4]Department of Physics, Kwame Nkrumah University of Science and Technology, Kumasi, Ghana
[5]Department of Basic Sciences, School of Basic and Biomedical Sciences, University of Health and Allied Sciences, Ho, Ghana

***Corresponding author: theazahgidi@gmail.com**

ABSTRACT

Ambient dose equivalent is determined at nine source-to-detector distances in a Secondary Standard Dosimetry Laboratory in a Cs-137 beam using a Physikalisch-Technische-Werkstaetten (PTW) ionisation chamber and Unidos electrometer as a measuring assembly. This work aims to estimate the gamma ambient dose equivalent resulting from air kerma rate distributions and subject the data generated to counting statistics to determine whether these data reflect proper instrument operation. The method of varying the source-to-detector distances was used. From the results, the total kinetic energy of all charged particles liberated by uncharged incident radiation per unit mass of material of the ionisation chamber ranged from 0.3168 ± 0.0146 µGy/s at an SSD of 1.0 m to 0.0151 ± 0.0007 µGy/s at 5.0 m within two standard deviations. The coefficient of variation among the various datasets ranged from 0.05% to 0.31%. Counting statistics of the generated data reflects proper measuring system operation and reliability. It is proposed that, in between calibrations, dosimetrists should consider relying upon counting statistics to check the output of their ionisation chambers for conformance to statistical laws.

Keywords: Air kerma, ambient dose equivalent, ionisation chamber, offset current

INTRODUCTION

Operational quantities in the field of health physics have been introduced to meet two other important needs besides standardization. These needs are operational measurement and estimation of radiation risk. The ambient dose equivalent, H*(10), is an operational quantity for area monitoring of ionising radiations. The operational dose equivalent quantity for area monitoring has been defined by the International Commission on Radiation Units and Measurements (ICRU) (ICRU, 1985, 1988, 1993, 2000). The International Commission on Radiological Protection (ICRP) Publication 103 defines H*(10) as the dose equivalent at a point in a radiation field that would be produced by the corresponding expanded and aligned field in the ICRU sphere at a depth of 10 mm on the radius vector opposing the direction of the aligned field (ICRP, 2007). The ICRU sphere is a sphere of tissue-equivalent material (30 cm in diameter, ICRU (soft) tissue with density: 1 g/cm^3, and mass composition: 76.2% oxygen, 11.1% carbon, 10.1% hydrogen, and 2.6% nitrogen). H*(10), therefore, denotes a deep radiation dose at a depth of 10 mm below the skin. It is particularly used to measure strongly penetrating gamma rays (above 12 keV) and neutrons (Harrison *et al*., 2021).

Kerma is an acronym for kinetic energy released per unit mass and is a measure of energy transferred from radiation to matter. Air kerma denotes the kinetic energy released per unit mass when a gamma beam is travelling through air. The basic use of air kerma in radiation metrology is in estimating ambient dose equivalent (Adjei et al., 2013; Azah et al., 2024). In interventional radiology, air kerma is used to estimate the (peak) skin dose to reduce the possibility of patient radiation burns due to high skin doses. (Balter et al., 2010; and Miller et al., 2010) Ambient dose equivalent is determined from air kerma and air kerma rates (Zeng et al., 2020; Mraity et al., 2021; Burns et al., 2006; Bor et al., 2004). Various methods for determining ambient dose equivalent for various applications and scenarios exist (Sato et al., 1999; Kuć, 2023; Leontaris et al, 2020; Casanovas et al., 2016; Elias et al., 2020; Poltabtim, 2023). Whilst NaI(TI) scintillation, and ionising chamber survey meters are used to measure gamma ray ambient dose rates on the field, Secondary Standard Dosimetry Laboratories (SSDLs) use ionisation chambers coupled with electrometers to determine H*(10) to provide traceability of field equipment to the international system of measurement.

The radiation detecting and measuring instruments used for radiation monitoring function are based on the mechanisms of interaction of radiation with matter. These mechanisms include compton scattering, photoelectric absorption, pair production, coherent scattering, etc. As a result, the operation of a particular radiation detector, fundamentally, depends on the nature of the radiation to be detected and how it interacts with the material construct of the detector. To get a good understanding of the response of a specific type of detector, one must be familiar with the mechanism by which different types of radiations interact with and lose their energy in different matter. An ideal instrument for determining ambient dose equivalent should have an isotropic response because it is required to measure H*(10) in any radiation field that is uniformly distributed over its dimensions.

Ionisation chambers, in principle, are the simplest of all gas-filled detectors (Knoll, 2010 and Greening, 2017) used to determine H*(10). Calibration is the main means of ensuring that an ionisation chamber is functioning well and producing data that is traceable to a primary standard (IAEA, 2008; ISO, 1993; Adjei et al., 2013; Azah et al., 2024). It takes more than a year for a secondary standard to be recalibrated. The reliability

of the performance of ionisation chambers (detectors in general) in between calibrations is a challenge to dosimetrists. The standard method of checking the measurement results of devices for conformance to statistical laws (Cerqueti et al., 2021; Hibbert, 2013; and Leblond, 2018) can be relied upon during these periods. This work aims to estimate the gamma ambient dose equivalent resulting from air kerma rate distributions at nine source-to-detector distances in a secondary standard dosimetry laboratory and subject the data generated to counting statistics to determine whether these data reflect proper instrument operation. The measured intensities of air kerma rates used in this work are emitted from a Ceasium-137 source.

MATERIAL AND METHODS

A PTW vented spherical ionisation chamber, Ceasium-137 gamma source assembly, PTW UNIDOS electrometer, thermometer, barometer, and a CCTV camera were used to conduct this study. The ionisation chamber is designed for the measurement of ionising radiations for radiation protection purposes. It has a sensitive volume of 1 L with the chamber centre as the reference point. Its spherical construct guarantees a near-uniform response to radiation from all directions. Figure 1 shows the outline of the ionisation chamber. It is ideal for measuring the quantities of air-kerma and photon equivalent doses. The nominal response of this chamber is 40 µC/Gy with a chamber voltage of 400 V nominal and ± 500 V maximal. The energy response and leakage current are in the range of ≤ ± 4 % and ≤ ± 10 fA respectively. The outer dimension of the chamber has a diameter of 140 mm. The walls of this chamber's sensitive volume are made of 3 mm polyoxymethylene (POM), 0.02 mm graphite, and 0.22 mm lacquer. This made the total wall area to have a density of 453 mg/cm^3.

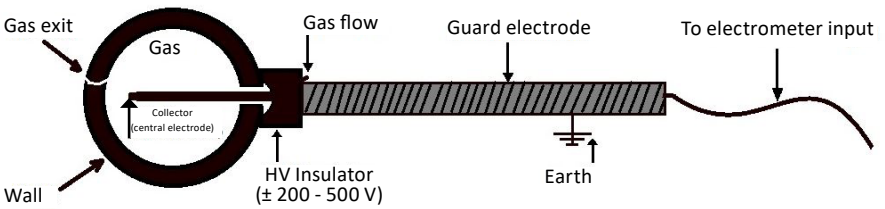

Figure 1. A spherical cavity ionisation chamber.

The chamber has a wall that is considered sufficiently thick to ensure that all the electrons crossing the air cavity originate in the wall and not in the surrounding material. The central electrode is a 50 mm diameter graphite-coated polystyrene. The ion collection efficiency at a nominal voltage for ≥ 90.0 % saturation is estimated at 420 mGy/h. The ionisation chamber was used together with PTW UNIDOS. It is a microprocessor-controlled universal reference class dosemeter. It is a very sensitive measuring equipment and a secondary standard for determining very low doses and dose rates in radiation protection, diagnostic radiology, and radiotherapy. It fulfils the general requirements for the safety of medical electrical equipment according to IEC 60601-1. As a universal reference class dosemeter, UNIDOS can display the measured values of current, charge, dose, and dose rate.

These features: high accuracy, long-term stability, excellent resolution, and wide

dynamic measuring ranges make UNIDOS an ideal dosemeter for this study.

Determination of Air Kerma rates and ambient dose equivalent

With the aid of a laser positioning system, the ionisation chamber is placed at a source-to-detector distance of 1 m and a spatial height of 1 m from the floor inside the calibration bunker. On the control console desk outside of the bunker, the UNIDOS electrometer was set up. Without connecting the two measuring devices, the positive high voltage (HV polarity +) switch at the rear of the UNIDOS was selected. This procedure prevents an accidentally too high a voltage from being applied to the ionisation chamber. The unit is then connected to the mains and powered on. Using the menu keys, the 1 L PTW ionisation chamber and its corresponding calibration factor were selected from the UNIDOS chamber library. The essence of the chamber library is that, before any measurement that UNIDOS does, it adjusts to a specific ionisation chamber and its details stored on it. It automatically checks for the quantity the chamber is calibrated for and goes ahead to provide the calibration factor whilst setting the high voltage to the last value used with the chamber successfully. This is possible because the calibration factors of the ionisation chambers are stored on the UNIDOS during their calibration at the primary standard dosimetry laboratory. In this study, the highest allowed chamber voltage of 400 V, a measuring mode of "dose" and a low range was selected. The set-up was allowed a period of 15 minutes to warm up. This is necessary for stabilising the offset current. The ionisation chamber was connected to the UNIDOS via an extension cable without switching off the latter. Since a low measuring range was selected, the set was again allowed a 15-minute waiting period for the electric potential to stabilise after the supply of the high voltage to the ionisation chamber. By pressing the integrating key (INT) on the front panel of the UNIDOS, the offset current value within 120 seconds was recorded. Ten offset current values were recorded. The ionisation chamber is now irradiated, and 10 charge measurements were made for 120 seconds each. The procedure is repeated at an SDD of 1.5 m and for seven more positions at an incremental distance of 0.5 m. In this work, the ionisation chamber-electrometer system was operated as an integrating-type counter and the effective point of measurement of the chamber is that which is displaced toward the source from the centre of the chamber.

The environmental conditions in the laboratory during the determination of the air kerma were different from those under which the ionisation chamber was calibrated in the primary standard dosimetry laboratory. The difference in the air densities could result in the variation of the number of ion pairs produced. The number of air molecules that the radiation field interacts with is dependent on the density of air in the sensitive volume of the ionisation chamber. Higher temperatures lower the density of the air in the chamber, and vice versa. The chamber reading therefore was corrected for temperature and pressure using Equation 1.

$$K_{TP} = \left(\frac{P_1}{P_2}\right)\left(\frac{273.15+T_2}{273.15+T_1}\right) \qquad \textbf{Eqn 1}$$

Where $\mathbf{K_{TP}}$ is the temperature-pressure correction factor, $\mathbf{P_1}$ and $\mathbf{T_1}$ are the pressure (in kPa) and temperature (in °C) conditions, respectively, under which the chamber was calibrated in a PSDL, and $\mathbf{P_2}$ and $\mathbf{T_2}$ are the temperature and pressure at which the air kerma rate measurements are made. The air kerma rates, $\mathbf{K_{air}}$, at the various SDDs were determined using the Equation 2.

$$\dot{K}_{\text{air}} = \frac{\text{Q}}{\text{t}} \text{ x } \text{K}_{\text{TP}} \text{ x } N_K \quad \textbf{Eqn 2}$$

where *Q* is the corrected charge collected at the ionisation chamber, ***t*** is the charge collecting interval, N_{K} is the air kerma calibration factor of the ionisation chamber and electrometer determined at a Primary Standard Dosimetry Laboratory. In this work, the ionisation chamber was operated in current mode as pulses were integrated over a fixed time of 120 seconds to give a continuous readout of the rate of ionisation.

The ambient dose equivalent is calculated using Equation 3

$$\text{H}^*(10) = h \text{ x } \dot{K}_{\text{air}} \quad \textbf{Eqn 3}$$

where ***h*** is the dose coefficient for caesium 137 and has the value of 1.21 Sv/Gy.

Counting statistics and uncertainty propagation

Radioactivity is a random process and measurements based on the observation of radiation emissions in nuclear disintegration experiments are prone to inherent statistical fluctuations. Additionally, data collection processes, ambient background radiations, and noise in the electronic components of the measuring system altogether represent an unavoidable source of measurement uncertainty. The quality control procedure of applying analytical methods can help to determine whether the internal fluctuation shown by multiple measurements is consistent with the amount of fluctuation expected should statistical fluctuations be the only source. By this path, abnormal amounts of fluctuation can be identified that could be indicative of malfunctioning of certain components of the counting system as well as indicate the repeatability of the measurement results.

From a generated data set of ***N*** independent measurements of the physical quantity $\boldsymbol{x}_{\text{i}}$, the sum, ***Σ***, is given by the expression in Equation 4.

$$\sum = \sum_{i=1}^{N} (x_i) \quad \textbf{Eqn 4}$$

To describe data with just a number, the best and most meaningful one to apply is the arithmetic mean, , given mathematically by Equation 5. (Knoll, 2010).

$$\bar{x} = \frac{\Sigma}{N} \quad \textbf{Eqn 5}$$

A sensible measure of the spread or dispersion about the mean is the sample variance, *(x),* and it is quantified using Equation 6

$$\sigma^2(x) = \frac{1}{N} \sum_{i=1}^{N} (x_i - \bar{x})^2 \quad \textbf{Eqn 6}$$

It should be noted that the mean value, $\bar{\text{x}}$, of a finite set of sample measurements differs from the true mean of the theoretical infinite population of measurements. As a result, there is an error in $\bar{\text{x}}$ used in the calculation of $\sigma^2(\text{x})$ in Equation 6 which tends to give a biased estimate of the variance of the infinite set of measurements. To better predict the variance of an infinite population, the Bessel correction factor (*N/N-1*) (Morris *et al*., 2012) is applied to Equation 6 to result in

$$\sigma^2(x) = \frac{1}{N-1} \sum_{i=1}^{N} (x_i - \bar{x})^2 \quad \textbf{Eqn 7}$$

where the term *N-1* is constant and known as the number of degrees of freedom. The

sample variance is the average squared deviation from the mean. The root mean squared deviation is known as the standard deviation, ***σ***, and is the square root of the variance. Equation 8 gives a reasonable estimate by which a particular data point differs from the mean.

$$\sigma = \sqrt{\frac{1}{N-1}\sum_{i=1}^{N}(x_i - \bar{x})^2} \qquad \textbf{Eqn 8}$$

The results from counting the ionisation events from a sample once can be expressed as

$$Counts = n \pm \sigma = n \pm \sqrt{n} \qquad \textbf{Eqn 9}$$

where ***n*** is the number of counts and ***σ=√n*** denotes one standard deviation applying Poisson statistics. For a sample counted for a specific period, the count rate is calculated using Equation 10

$$Count\ Rate = \frac{n_s}{t_s} \pm \frac{\sqrt{n}}{t_s} = C_s \pm \sqrt{\frac{C_s}{t_s}} \qquad \textbf{Eqn 10}$$

Where $\mathbf{t_s}$ is the sample counting time and $C_s = {}^{n_s}/_{t_s}$ (sample count per unit time). It is worth noting that the variance of the difference of two independent variables is the sum of their variances.

Thus, for sample dataset,

$$\sigma_s^2 = \sigma_t^2 + \sigma_b^2 \qquad \textbf{Eqn 11}$$

given that σ_s^2 is the sample variance, σ_t^2 is the total variance σ_b^2 is the background variance. The standard deviation of the sample may then be expressed as (ICRU, 1993)

$$\sigma_s = \sqrt{\frac{n_s + n_b}{t_t^2} + \frac{n_b}{t_b^2}} \qquad \textbf{Eqn 12}$$

This reduces to

$$\sigma_s = \sqrt{\frac{C_t}{t_t} + \frac{C_b}{t_b}} \qquad \textbf{Eqn 13}$$

where $\boldsymbol{C_t}$ is the gross count rate and $\boldsymbol{C_b}$ is the background count rate. The direct measurement result is then stated as

$$Charge\ collected = C_s \pm \sqrt{\frac{C_t}{t_t} + \frac{C_b}{t_b}} \qquad \textbf{Eqn 14}$$

The uncertainty associated with the determination of the ambient dose equivalent in this study was estimated using methods recommended by Lewis *et al* (2005), IAEA (IAEA, 2008) and the International Standard Organization (ISO) (ISO, 1993).

$$\frac{U_{H^*(10)}}{H^*(10)} = \sqrt{\left(\frac{U_Q}{Q}\right)^2 + \left(\frac{U_{KTP}}{K_{TP}}\right)^2 + \left(\frac{U_{N_K}}{N_K}\right)^2 + \left(\frac{U_h}{h}\right)^2} \qquad \textbf{Eqn 15}$$

where $\boldsymbol{U_{H^*(10)}}$ is the uncertainty of the ambient dose equivalent; $\boldsymbol{U_Q}$ is the uncertainty component of the mean reading of the ionisation chamber in establishing the air kerma free-in-air; $\boldsymbol{U_h}$ is the uncertainty of the dose conversion coefficient, and this includes calibration using the ^{137}Cs and $\boldsymbol{U_{NK}}$ is the uncertainty component of the standard ionisation chamber calibration (referred from the calibration certificate). An overall expanded uncertainty in the calibration of a survey meter for 95 % confidence probability is expressed as a product of the standard uncertainty and a coverage factor of k = 1.96 (ISO, 1993). In expressing the final measurement uncertainty, the value and its

uncertainty were rounded off to the same precision.

RESULT AND DISCUSSION

The ionisation chamber used had low offset (leakage) current. The largest leakage was 0.062% of the maximum signal. The offset current values measured are shown in Table 1. To prevent the production of spurious ionisation current because of irradiating the chamber's stem, collecting electrode, or cable with high-energy electrons, the source-to-detector distance of 5 m was not exceeded. Beyond an SDD of 5 m, the field size is sufficiently large enough to irradiate the stem. As a result, stem and cable effects were negligible. The measured charges accumulated by the measuring system during the air kerma determination were precise and shown in Table 2 as a function of distance from the radiation source. It ranged from a maximum of 1505.0 ± 0.7 pC/120s to a minimum of 72.0 ± 0.2 pC/120s. The net count rate is captured in Table 3 ranging from 0.60 ± 0.07 pC/s to 12.53 ± 0.32 pC/s. The charge distribution relative to the various SSD approximated an inverse square law pattern.

Table 1: Offset current in pico coulomb (pC) collected within 120 s at various SDD

1.0 m	1.5 m	2.0 m	2.5 m	3.0 m	3.5 m	4.0 m	4.5 m	5.0 m
0.21±0.05	1.09±0.06	0.04±0.11	0.24±0.18	0.13±0.19	2.31±0.55	0.45±0.05	0.92±0.22	0.46±0.08
0.20±0.05	0.94±0.06	0.10±0.11	0.50±0.18	0.41±0.19	0.39±0.55	0.41±0.05	1.17±0.22	0.62±0.08
0.25±0.05	0.97±0.06	0.33±0.11	0.50±0.18	0.53±0.19	0.44±0.55	0.31±0.05	1.06±0.22	0.56±0.08
0.19±0.05	0.95±0.06	0.19±0.11	0.58±0.18	0.76±0.19	0.49±0.55	0.33±0.05	0.78±0.22	0.50±0.08
0.25±0.05	0.90±0.06	0.36±0.11	0.49±0.18	0.71±0.19	0.77±0.55	0.40±0.05	0.38±0.22	0.53±0.08
0.28±0.05	0.91±0.06	0.13±0.11	0.53±0.18	0.64±0.19	0.92±0.55	0.43±0.05	0.61±0.22	0.47±0.08
0.28±0.05	0.91±0.06	0.07±0.11	0.65±0.18	0.68±0.19	0.93±0.55	0.35±0.05	0.73±0.22	0.41±0.08
0.17±0.05	0.87±0.06	0.13±0.11	0.78±0.18	0.49±0.19	0.76±0.55	0.44±0.05	0.72±0.22	0.53±0.08
0.29±0.05	0.86±0.06	0.09±0.11	0.85±0.18	0.53±0.19	0.64±0.55	0.34±0.05	0.81±0.22	0.40±0.08
0.17±0.05	0.92±0.06	0.18±0.11	0.72±0.18	0.67±0.19	0.67±0.55	0.39±0.05	0.75±0.22	0.38±0.08

Table 2: Charges collected within the collection period of 120 s in pico coulomb (pC) at various SDD

1.0 m	1.5 m	2.0 m	2.5 m	3.0 m	3.5 m	4.0 m	4.5 m	5.0 m
1505.0±0.7	770.0±0.2	378.5±0.5	291.0±0.5	215.5±0.2	161.0±0.3	127.0±0.3	88.0±0.4	72.0±0.2
1506.0±0.7	770.5±0.2	378.5±0.5	292.5±0.5	215.5±0.2	161.5±0.3	127.0±0.3	87.5±0.4	72.5±0.2
1505.0±0.7	770.5±0.2	380.0±0.5	293.0±0.5	215.0±0.2	161.0±0.3	127.0±0.3	87.5±0.4	72.5±0.2
1504.0±0.7	770.5±0.2	379.0±0.5	292.0±0.5	215.5±0.2	160.5±0.3	126.5±0.3	87.0±0.4	72.5±0.2
1504.0±0.7	770.5±0.2	379.0±0.5	292.5±0.5	215.5±0.2	160.5±0.3	126.5±0.3	87.0±0.4	72.5±0.2
1504.0±0.7	770.5±0.2	379.0±0.5	292.5±0.5	215.5±0.2	161.0±0.3	127.0±0.3	87.0±0.4	72.0±0.2
1504.0±0.7	770.5±0.2	379.0±0.5	292.5±0.5	215.0±0.2	161.0±0.3	126.5±0.3	87.0±0.4	72.0±0.2
1504.0±0.7	770.0±0.2	379.5±0.5	292.5±0.5	215.5±0.2	160.5±0.3	126.5±0.3	87.5±0.4	72.5±0.2
1504.0±0.7	770.0±0.2	379.5±0.5	292.5±0.5	215.5±0.2	160.5±0.3	126.5±0.3	87.0±0.4	72.5±0.2
1504.0±0.7	770.5±0.2	379.5±0.5	292.5±0.5	215.0±0.2	160.5±0.3	126.5±0.3	87.0±0.4	72.5±0.2

Table 3: Net count rate reported with a 2σ

pC/s								
1.0 m	**1.5 m**	**2.0 m**	**2.5 m**	**3.0 m**	**3.5 m**	**4.0 m**	**4.5 m**	**5.0 m**
12.54 ± 0.64	6.41 ± 0.46	3.15 ± 0.32	2.42 ± 0.28	1.79 ± 0.24	1.32 ± 0.22	1.05 ± 0.18	0.73 ± 0.08	0.60 ± 0.14
12.55 ± 0.64	6.41 ± 0.46	3.15 ± 0.32	2.43 ± 0.28	1.79 ± 0.24	1.34 ± 0.22	1.05 ± 0.18	0.72 ± 0.08	0.60 ± 0.14
12.54 ± 0.64	6.41 ± 0.46	3.16 ± 0.32	2.44 ± 0.28	1.79 ± 0.24	1.34 ± 0.22	1.06 ± 0.18	0.72 ± 0.16	0.60 ± 0.14
12.53 ± 0.64	6.41 ± 0.46	3.16 ± 0.32	2.43 ± 0.28	1.79 ± 0.24	1.33 ± 0.22	1.05 ± 0.18	0.72 ± 0.16	0.60 ± 0.14
12.53 ± 0.64	6.41 ± 0.46	3.16 ± 0.32	2.43 ± 0.28	1.79 ± 0.24	1.33 ± 0.22	1.05 ± 0.18	0.72 ± 0.16	0.60 ± 0.14
12.53 ± 0.64	6.41 ± 0.46	3.16 ± 0.32	2.43 ± 0.28	1.79 ± 0.24	1.33 ± 0.22	1.05 ± 0.18	0.72 ± 0.16	0.60 ± 0.14
12.53 ± 0.64	6.41 ± 0.46	3.16 ± 0.32	2.43 ± 0.28	1.79 ± 0.24	1.33 ± 0.22	1.05 ± 0.18	0.72 ± 0.16	0.60 ± 0.14
12.53 ± 0.64	6.41 ± 0.46	3.16 ± 0.32	2.43 ± 0.28	1.79 ± 0.24	1.33 ± 0.22	1.05 ± 0.18	0.72 ± 0.16	0.60 ± 0.14
12.53 ± 0.64	6.41 ± 0.46	3.16 ± 0.32	2.43 ± 0.28	1.79 ± 0.24	1.33 ± 0.22	1.05 ± 0.18	0.72 ± 0.16	0.60 ± 0.14
12.53 ± 0.64	6.41 ± 0.46	3.16 ± 0.32	2.43 ± 0.28	1.79 ± 0.24	1.33 ± 0.22	1.05 ± 0.18	0.72 ± 0.16	0.60 ± 0.14

The total kinetic energy of all charged particles liberated by uncharged incident radiation per unit mass of material of the ionisation chamber ranged from 0.3168 ± 0.0146 µGy/s at an SSD of 1.0 m to 0.0151 ± 0.0007 µGy/s at 5.0 m. Table 4 displays the environmental conditions at the time of charge collection.

In Figure 2, the determined H*(10) values were plotted as a function of nine SSD. Table 5 estimates the uncertainty associated with the determination of the ambient dose equivalent in this study. The air kerma rates determined in this study are comparable to those determined by Adjei et al (2013) and Azah et al (2024) using the same set of measurement assembly, confirming further the reliability of the secondary standard.

Table 4. Environmental conditions associated with the determination of H*(10)

SDD/m	Average Chamber Reading [pC/s]	K_{air} [µGy/s]	H*(10) [mSv/h]	Average Temperature /°C	Average Pressure /kPa	Relative Humidity	K_{Tp}
1.0	12.53 ± 0.32	0.3168 ± 0.0146	1.3798 ± 0.0635	23.55±0.34	102.30±0.16	41.50±0.53	1.0020±0.0027
1.5	6.41 ± 0.23	0.1619 ± 0.0074	0.7053 ± 0.0324	23.35±0.34	102.00±0.16	41.35±0.53	1.0013±0.0027
2.0	3.16 ± 0.16	0.0801 ± 0.0037	0.3490 ± 0.0161	24.10±0.34	102.10±0.16	40.40±0.53	1.0059±0.0027
2.5	2.43 ± 0.14	0.0616 ± 0.0028	0.2684 ± 0.0123	23.55±0.34	102.05±0.16	41.40±0.53	1.0050±0.0027
3.0	1.79 ± 0.12	0.0454 ± 0.0021	0.1978 ± 0.0091	23.25±0.34	101.95±0.16	41.30±0.53	1.0057±0.0027
3.5	1.33 ± 0.11	0.0339 ± 0.0016	0.1478 ± 0.0068	23.80±0.34	101.70±0.16	41.60±0.53	1.0089±0.0027
4.0	1.05 ± 0.09	0.0267 ± 0.0012	0.1163 ± 0.0053	23.35±0.34	101.90±0.16	41.35±0.53	1.0054±0.0027
4.5	0.72 ± 0.08	0.0183 ± 0.0008	0.0798 ± 0.0037	24.20±0.34	101.95±0.16	41.25±0.53	1.0083±0.0027
5.0	0.60 ± 0.07	0.0151 ± 0.0007	0.0659 ± 0.0030	23.85±0.34	101.90±0.16	40.05±0.53	1.0018±0.0027

Table 5: Estimated relative standard uncertainty

Influence quantity	Distribution	Type	Relative standard uncertainty, u (%)	Sensitivity coefficient, c	Uncertainty component, c x u (%)
Reference standard					
Calibration from PSDL	Gaussian	B	1.50	1	1.50
Long term stability of the secondary standard	Gaussian	A	0.17	1	0.17
Change in source position	Gaussian	B	0.1	1.41	0.07
Temperature change	Rectangular	B	0.02	1	0.02
Pressure change	Rectangular	B	0.1	1	0.10
Reference air kerma measurements - repeatability	Gaussian	A	0.05	1	0.05
Reference air kerma measurements - resolution	Rectangular	B	0.1	0.32	0.31
Device positioning	Rectangular	B	0.05	2	0.01
Overall relative uncertainty					2.23
Relative expanded uncertainty (k = 2)					**4.46**

The fact that radiations produce ions upon interactions with matter, and that these ions multiply in a sufficiently high electric field (Ouseph, 1975) is the basis of this study. The measuring system chosen for this work produced precise measurements at all SSDs. Since in counting experiments, the true value is assumed to be the arithmetic mean, a measure of the accuracy of the data generated is then the amount that each determined value deviates from the mean. From Table 1 and Table 2, the sample count rates are large compared to the background radiation (offset current). This condition makes the standard deviation of the datasets an adequate descriptor. The standard deviation of measurements made at the SSD of 1 m are the largest at 0.32. The least sample standard deviation of 0.07 occurred among data generated at an SSD of 5.0 m. The plotted values of the ambient dose equivalent against SDD in Figure 2 generally approximates the inverse square law. It shows that the radiation flux is inversely proportional to the square of the distance from the point source. In radiation protection, the inverse square law plays a critical role. It determines the safe distance a person must keep from a source to minimize, as low as reasonably achievable (ALARA), the exposure and possibility of radiation damage. It is observed from Figure 2 that the experimentally generated data for H*(10) best fits the theoretical trend at an SSD of 2.0 m and beyond. At SSD less than 2.0 m, the curve is not smooth and noticeably, slightly deviated from the trend curve. The concept of cross-section can offer some insights into this observation.

The cross section in particle physics, as it relates to this study, is a measure of the likelihood that the flux will collide with particles of air in the sensitive volume of the ionisation chamber and has a standard unit of barn quantified as either 10^{-28} m² or 10^{-24} cm². In physical terms, cross-section can be viewed as a characteristic area where a larger area means a greater probability of interaction. Error due to device positioning in the beam could have affected the cross section at SSD less than 2.0 m. However, at SSD of 2.0 m and more, the flux completely engulfs the sphere of the ionisation chamber increasing the probability of interactions.

The coefficient of variation among the various datasets ranged from 0.05% to 0.31%. The very low values imply that relative to the mean, variability in the measurements is low and the measurements are reasonably consistent. With this low variability, the measures of central tendency can be regarded as a dependable guide to the representative performance of the measuring system. Table 4 displays the descriptive statistics of the measurement. The uncertainties stated in this work are within the same range as stated by Azah et. al. (2024) and Adjei et. al. (2023) who carried out some earlier studies using the same measurement system. Azah *et al*'s maximum uncertainty was ±18.1% within two standard deviations and Adjei *et al* propagated uncertainties between 0.5% to 17.0%.

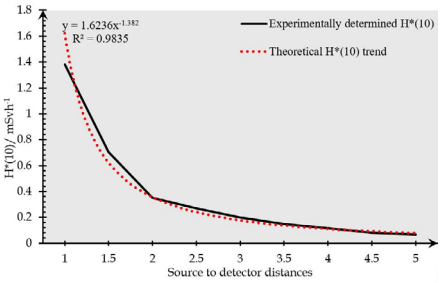

Figure 2. A plot of ambient dose equivalent at selected SDD

Table 6: Descriptive statistics of sample charges collected at various SSD

Parameter	Sample charges								
	1.0 m	1.5 m	2.0 m	2.5 m	3.0 m	3.5 m	4.0 m	4.5 m	5.0 m
Sample Standard deviation	0.0059	0.0021	0.0036	0.0038	0.0028	0.0052	0.0021	0.0024	0.0019
Sample mean	12.53	6.41	3.16	2.43	1.79	1.33	1.05	0.72	0.60
Standard deviation of the mean	0.0019	0.0007	0.0011	0.0012	0.0009	0.0016	0.0007	0.0008	0.0006
Minimum	12.53	6.41	3.15	2.42	1.79	1.32	1.05	0.72	0.60
Maximum	12.55	6.41	3.16	2.44	1.79	1.34	1.06	0.73	0.60
Coefficient of variation	0.05	0.03	0.11	0.16	0.16	0.39	0.20	0.33	0.31

CONCLUSION

The gamma ambient dose equivalent resulting from air kerma rate distributions at nine source-to-detector distances has been estimated in the SSDL and the results follow the inverse square rule. Subjecting the data generated to counting statistics, the number of measurements with a small error is much larger than the number of measurements with a relatively large error. This is a confirmation that the mean value of the measurements made at each source-to-detector distance gets closer to the true value as the standard deviation decreases. The very low standard error of the mean, from Table 6, estimates that the difference between the sample mean value of a finite set of measurements at a particular SDD and the mean of an infinite data set measured at the same SDD is very small. We conclude that the data obtained from this study reflect proper measuring system operation and is reliable. It is proposed here that, in between

calibrations, dosimetrists should consider relying upon counting statistics to check the output of their ionisation chambers for conformance to statistical laws. It is recommended that in determining ambient dose equivalent using a variable source-to-detector distance method, the distances apart should be less than 0.5 m used in this work. This will result in a smoother curve when data is plotted and reveal more detailed insights.

Data availability

The data underlying this article are available in the article.

ACKNOWLEDGEMENTS

The authors acknowledge the Radiation Protection Institute of the Ghana Atomic Energy Commission for providing the resources used in this work.

Declaration of conflict of interest

The authors have no conflict of interest to declare.

REFERENCES

Adjei, D., Darko, E. O., Schandorf, C., Owusu-Manteaw, P. & Akrobortu, E. (2013). Analysis of calibration results of radiation survey meters used for area monitoring. *Radiation. Protection. Dosimetry,* 152(4): 273–278

Azah, C. K, Deatanyah, P., Appiah, P. M., Osei, S., Amoako, J. K., and Sam, F. (2024). Evaluation of calibration factors of digital survey meters in a secondary standard dosimetry laboratory. *Radiation Protection Dosimetry*, 200(2): 113–119

Balter, S., Hopewell, J.W., Miller, D.L., Wagner, L.K. and Zelefsky, M.J. (2010). Fluoroscopically guided interventional procedures: A review of radiation effects on patients' skin and hair. *Radiology.* 254(2): 326-341.

Bor, D., Sancak, T., Olgar, T.U.R.A.N., Elcim, Y., Adanali, A., Sanlidilek, U. and Akyar, S. (2004). Comparison of effective doses obtained from dose–area product and air kerma measurements in interventional radiology. *British Journal of Radiology*. 77(916): 315-322

Burns, D.T. (2006). A new approach to the determination of air kerma using primary-standard cavity ionisation chambers. *Physics in Medicine & Biology*. 51(4): 929. https://doi.org/10.1088/0031-9155/51/4/012

Casanovas, R., Prieto, E. & Salvadó, M. (2016). Calculation of the ambient dose equivalent H*(10) from gamma-ray spectra obtained with scintillation detectors. Applied Radiation and Isotopes 118: 154-159. https://doi.org/10.1016/j.apradiso.2016.09.001

Cerqueti, R., & Maggi, M. (2021). Data validity and statistical conformity with Benford's Law. *Chaos, Solitons & Fractals*. 144: 110740.

Elias, C.C.R., D'Oliveira Cardoso, D., de Medeiros, M.P.C., de Oliveira, C.L., Gavazza, S., Correa, S.C.A. & Souza, E.M. (2020). Evaluation of Ambient Dose Equivalent Surrounding Transmission Full-Body Scanners. *Radiation Protection Dosim*etry, 189(4): 444-451. https://doi.org/10.1093/rpd/ncaa066

Greening, J. R. (2017). Fundamentals of radiation dosimetry. CRC Press.

Harrison, J. D., Balonov, M., Bochud, F., Martin, C. J., Menzel, H.-G., Smith-Bindman, R., Hibbert, D.B. (2013). Evaluation of measurement data: The role of measurement uncertainty in conformity assessment. *Chemistry International*, 35(2): 22-23.

International Atomic Energy Agency (2008). Measurement Uncertainty: A practical guide for secondary standards dosimetry laboratories (TECDOC-1585). International Atomic Energy Agency.

International Commission on Radiological Protection. (2007). Recommendations of the International Commission on Radiological Protection(ICRP Publication 103. Pergamon Press.

International Commission on Radiation Units and Measurements. (1985). Determination of dose equivalents resulting from external radiation sources. (ICRU Report 39). International Commission on Radiation Units and Measurements

International Commission on Radiation Units and Measurements.(1988). Determination of dose equivalents from external radiation sources – Part II.(ICRU Report 43). International Commission on Radiation Units and Measurements.

International Commission on Radiation Units and Measurements (1993). Quantities and units in radiation protection dosimetry. (ICRU Report 51). International Commission on Radiation Units and Measurements

International Commission on Radiation Units and Measurements.(2020). Operational Quantities for External Radiation Exposure. (ICRU Report 95). International Commission on Radiation Units and Measurements.

International Organization for Standardization. (1993). Guide to the expression of uncertainty in measurement. International Organization for Standardization.

Knoll, G.F. (2010). Radiation Detection and Measurement, 4th ed. Wiley

Kuć, M. (2023). Fast method of determining the ambient dose equivalent at a depth of 10mm of gamma-neutron fields based on recombination methods. *Radiation Protection Dosimetry*. *199*(15-16): 1872-1876 https://doi.org/10.1093/rpd/ncad016

Leblond, L. & Pillet, M. (2018). Conformity and statistical tolerancing. *International Journal of Metrology and Quality Engineering*. 9(1) 1.

Leontaris, F., Boziari, A., Clouvas, A., Kolovou, M. and Guilhot, J. (2020). Procedures to measure mean ambient dose equivalent rates using electret ion chambers. *Radiation Protection Dosimetry*. *190*(1): 6-21. https://doi.org/10.1093/rpd/ncaa061

Lewis, V. E., Woods, M. J., Burgess, P., Green, S., Simpson, J. and Wardle, J. (2005). Measurement Good Practice Guide: No. 49: the assessment of uncertainty in radiological calibration and testing. National Physical Laboratory, Middlesex https://eprintspublications.npl.co.uk/2793/

Miller, D.L., Balter, S., Schueler, B.A., Wagner, L.K., Strauss, K.J. and Vañó, E., (2010).

Clinical radiation management for fluoroscopically guided interventional procedures. *Radiology*. 257(2): 321-332.

Morris, A. S., and Langari, R. (2012). Measurement and Application: theory and application

Academic, California Mraity, H.A.A., and Al Aseebee, M.K. (2021). Evaluation of Entrance Surface Air Kerma in Patients During PA Chest Radiography Using CALDose Program in Al Najaf Governorate Hospitals. *Journal of Physics: Conference Series*. 1963(1): 012035

Ortiz-López, P., Simmonds, J. R., and Wakeford, R. (2021). The use of dose quantities in radiological protection: ICRP publication 147 Ann ICRP 50(1). *J. Radiol. Prot.* 41(2): 410-417 https://doi.org/10.1088/1361-6498/abe548

Ouseph, P. J., (1975). Introduction to Nuclear Radiation Detectors. Plenum Press, New York.

Poltabtim, W., Musikawan, S., Thumwong, A., Omori, Y., Kranrod, C., Hosoda, M., Saenboonruang, K. and Tokonami, S. (2023). Estimation of ambient dose equivalent rate distribution map using walking survey technique in Hirosaki City, Aomori, Japan. *Int J Environ Res Public Health*. 20(3): 2657. https://doi.org/10.3390/ijerph20032657

Sato, O., Yoshizawa, N., Takagi, S., Iwai, S., Uehara, T., Sakamoto, Y., Yamaguchi, Y. And Tanaka, S.I. (1999). Calculations of effective dose and ambient dose equivalent conversion coefficients for high energy photons. *Journal of nuclear science and technology*, *36*(11): 977-987.

Zeng, J., Qu P., Pang Q., and Wang. P. (2020). The Measurement of the Air-Kerma Rate in Air and a Solid Phantom with Ionization Chambers for a 192Ir HDR Brachytherapy Source. *Cancer Management and Research*. 12(2020): 10821-10828. https://www.tandfonline.com/doi/full/10.2147/CMAR.S275378#d1e158